



PCCP

Degradation of NTO induced by superoxide and hydroperoxyl radical: Comprehensive DFT study

| | |
|-------------------------------|---|
| Journal: | <i>Physical Chemistry Chemical Physics</i> |
| Manuscript ID | CP-ART-11-2023-005603 |
| Article Type: | Paper |
| Date Submitted by the Author: | 17-Nov-2023 |
| Complete List of Authors: | Sviatenko, Liudmyla; Donec'kyj nacional'nyj medychnyj universytet imeni M Hor'koho, General and Biological Chemistry N2 Gorb, Leonid; Institute of Molecular Biology and Genetics National Academy of Sciences of Ukraine, Quantum and Molecular Biophysics Leszczynski, Jerzy; Jackson State University, Department of Chemistry |
| | |

SCHOLARONE™
Manuscripts

ARTICLE

Degradation of NTO induced by superoxide and hydroperoxyl radical: Comprehensive DFT study

Liudmyla K. Sviatenko,^a Leonid Gorb^{b,c} and Jerzy Leszczynski^{*a}

Received 00th January 20xx,
Accepted 00th January 20xx

DOI: 10.1039/x0xx00000x

Reactive oxygen species, produced in the aquatic environment under sunlight irradiation, actively take part in degradation of environmental pollutants. NTO (5-nitro-1,2,4-triazol-3-one), being a primary ingredient in a suite of insensitive munitions formulations, may be released onto training range soils after incomplete detonations and dissolved in surface water and groundwater due to good water solubility. A detailed investigation of possible mechanism for NTO decomposition in water induced by superoxide and hydroperoxyl radical as one of the pathway for NTO environmental degradation was performed by computational study at PCM(Pauling)/M06-2X/6-311++G(d,p) level. Superoxide causes rapid deprotonation of NTO. Decomposition of NTO induced by hydroperoxyl radical was found to be a multistep process leading to mineralization of nitrocompound. The reaction process may begin with hydroperoxyl radical attachment to carbon atom of C=N double bond of NTO, then proceeds through rupture of C-N bonds and addition of water molecules leading to formation of nitrous acid, ammonia, nitrogen gas, hydrazine, and carbon (IV) oxide. The obtained results indicate that the anionic form of NTO shows a higher reactivity towards hydroperoxyl radical than its neutral form. Excitation of NTO by sunlight enables complete mineralization of NTO induced by superoxide. Calculated activation energies and exergonicity of the studied processes support contribution of hydroperoxyl radical and superoxide to degradation of NTO in environment into low-weight inorganic compounds.

Introduction

Highly energetic substances, used as explosive materials, cause pollution when they enter the environment, creating a toxic hazard for the biota. All over the world, soils and natural waters are contaminated with such pollutants due to munitions dumping, military activities, industrial operations etc. NTO (5-nitro-1,2,4-triazol-3-one) is a powerful insensitive explosive, present in industrial waste waters as well as in training fields.¹ Variety of possible pathways of NTO decomposition in environment make it of considerable interest for investigation to both experimental and computational chemistry. NTO dissolves easily in surface water and groundwater due to a good water solubility² and undergoes photo-transformation, which is a complex process that involves direct and indirect photolysis.³⁻⁸ Direct photolysis is considered as a hydrolytic decomposition of NTO in triplet state. Indirect photolysis of NTO involves reactions with reactive oxygen species (singlet oxygen, superoxide, hydroperoxyl radical, hydroxyl radical etc.), generated in water solution under UV-irradiation. The identified aqueous products of NTO photo-transformation are nitrite, nitrate, ammonium and 5-hydroxy-1,2,4-triazol-3-one or 1,2,4-triazolidine-3,5-dione – its isomer.³⁻⁸ Understanding of the mechanism of direct and indirect photochemical degradation of NTO is necessary in order to predict and control its environmental fate and persistence. Reactions of direct photolysis of NTO and its decomposition induced by singlet oxygen were modeled recently.^{9,10} In the present study we examine ability of superoxide and hydroperoxyl radical take part in degradation of NTO. Superoxide ($O_2^{\bullet-}$), as a one of reactive species, may be produced as a result of the donation of an electron to oxygen by photosensitizer after absorption of light.¹¹ The conjugate acid of the superoxide is a hydroperoxyl radical (HO_2^{\bullet}), which is produced upon sunlight irradiation of components such as dissolved organic matter (DOM), nitrate, nitrite, and Fe(III) present in natural waters. It plays important role in decomposition of organic pollutants.¹²⁻¹⁴ Hydroperoxyl radical is a stronger oxidant than superoxide, that is consistent with the experimental reduction potentials of 1.06 and 0.94 eV for HO_2^{\bullet} and $O_2^{\bullet-}$, respectively.¹⁴ An experimental pKa of 4.88 indicates that in neutral pH the major form of the superoxide reactant is the anionic form.¹⁵

^a Interdisciplinary Center for Nanotoxicity, Department of Chemistry, Physics & Atmospheric Sciences, Jackson State University, Jackson, Mississippi, 39217, USA.

^b Institute of Molecular Biology and Genetics, NAS of Ukraine, 150 Zabolotny Str., Kyiv, 03143, Ukraine.

^c QSAR Lab Sp. z o.o. Trzy Lipy 3, B, Gdansk, 80-172, Poland.

Electronic Supplementary Information (ESI) available: Optimized structures of transition states for NTO decomposition in water under action of superoxide and hydroperoxyl radical. Cartesian coordinates for optimized local minima and transition states species. See DOI: 10.1039/x0xx00000x

The investigation of reactivity of several classes of organic compounds in nucleophilic substitution reactions with superoxide showed that the nucleophilic attack of $O_2^{\cdot-}$ at the O-alkyl carbon is a common mechanism of decomposition of organic carbonates, aliphatic carboxylic esters, lactones. However, N-alkyl substituted amides, lactams, and ethers (glymes) are stable against nucleophilic substitution by superoxide.¹⁶ Nucleophilic reactions of $O_2^{\cdot-}$ with phenol esters of carboxylic acids proceed via attack at the carbonyl carbon.¹⁶ A one-electron transfer from $O_2^{\cdot-}$ was found as the major reaction channel for reaction of superoxide with 2,4,6-trinitrotoluene, while the proton abstraction reaction was negligible, which interestingly, is in contrast to the observed deprotonation of 2,4-dinitrotoluene, 2-nitrotoluene, and quercetin.^{17,18} Reaction of superoxide with 5,5-dimethyl-1-pyrroline *N*-oxide occurs by an addition of $O_2^{\cdot-}$ to carbon atom of the double C=N bond.¹⁹ The addition of HO_2^{\cdot} to 5,5-dimethyl-1-pyrroline *N*-oxide is predicted to be more exoergic with lower energy barrier than the addition of $O_2^{\cdot-}$. This is experimentally confirmed. The hydrogen atom abstraction and radical adduct formation were suggested as possible initial reaction routes between HOO^{\cdot} and coumarin derivatives.¹³

The current study is aimed to model NTO degradation induced by superoxide and hydroperoxyl radical in aqueous solution to evaluate possibility of NTO mineralization. Based on the structure of NTO and available literature data on mechanisms of reactions of superoxide and hydroperoxyl radical with different classes of organic compound^{13,14,16-19} the three directions for the reaction between superoxide and NTO will be considered: the nucleophilic attack of $O_2^{\cdot-}$ onto two carbon atoms of NTO, the deprotonation of NTO, and the one-electron transfer from $O_2^{\cdot-}$. The three pathways will also be discussed for reaction of hydroperoxyl radical with NTO: the attachment of HO_2^{\cdot} to carbon atoms of NTO, the hydrogen atom transfer from NTO to HO_2^{\cdot} , and the one-electron transfer from HO_2^{\cdot} . The studied reactions will be modeled for NTO and its anion (NTOa). NTO deprotonated at N4 position was chosen for calculation due to its increased stability as compared with NTO deprotonated at N2 position.²⁰

Methods

The geometries of all structures were optimized within the Gaussian 09 program²¹ using the M06-2X functional of the Density Functional Theory (DFT) and 6-311++G(d,p) basis set.²²⁻²⁵ M06-2X functional was recommended for applications involving thermochemistry, kinetics, and noncovalent interactions on the base of assessment of its performance over broad amounts of data.²² The influence of water bulk was simulated within PCM model in a combination with Pauling radii.²⁶ Stationary points for modeled reactions were characterized as either local minima (reactant, intermediate, product) having all real frequencies, or as transition states possessing only one imaginary frequency. This was carried out by calculation of the analytic harmonic vibrational frequencies at the PCM(Pauling)/M06-2X/6-311++G(d,p) theory level. The activation energy for electron transfer was calculated from Marcus theory using the internal reorganization energies and the reaction Gibbs free energies.²⁷ The Cartesian coordinates for optimized local minima and transition states species are provided in ESI.

Results and discussion

Superoxide induced degradation of NTO and NTOa

Considered in this paper reactions of NTO with superoxide in water along with the corresponding Gibbs free energy diagram are shown in Fig. 1. Structures of the corresponding transition states are placed in Fig. S1 (ESI). There are several possible directions for the initial attack of superoxide onto NTO. They are superoxide attachment to carbon atom of NTO, proton detachment from NTO, electron transfer from superoxide to NTO. The possibility of superoxide addition to the C3 carbon atom can be excluded, because this would lead to intermediate INT1 lying 41.39 kcal/mol above the reactants. Obtained high activation energy for attachment of superoxide to carbon atom of carbonyl group corresponds to the values reported in the study of mechanism of reaction between superoxide and organic carbonates, aliphatic carboxylic esters, lactones.¹⁵ An addition of superoxide to carbon atom C5 requires activation energy of 25.03 kcal/mol, which might not be easily accessible at room temperature. Once this transition state is reached, unstable INT2 undergoes nearly barrierless exergonic C-N bond rupture leading to nitrite anion release.

An electron transfer from superoxide to NTO is easy to proceed with formation of INT3, which is an anion radical of NTO. Unimolecular and hydrolytic decomposition of INT3 will not be realized due to high energy barriers that was studied earlier.²⁸ A hydrogen atom transfer from INT3 to superoxide is barrierless process. A hydrogen atom removal from atom 4 of INT3 is more favorable than from position 2 and leads to NTOa. An addition of superoxide to carbon atom C3 of INT3 will not be realized due to high instability of formed intermediate INT5. An attack of superoxide onto carbon atom C5 of INT3 requires high activation energy of 33.90 kcal/mol.

Proton transfer from nitrogen atom N4 of NTO to superoxide is more favorable than a proton transfer from N2 atom of NTO and leads to more stable NTOa and hydroperoxyl radical. Based on obtained results deprotonation of NTO in position 4 is the most energy favorable process for the reaction of NTO with superoxide. Further possible degradation of NTOa induced by superoxide and hydroperoxyl radical will be discussed below.

Various reactions of superoxide with anion of NTO were studied. They are attachment of superoxide to carbon atom of NTOa, proton detachment from NTOa, and electron transfer from superoxide to NTOa. Gibbs free energy profile for reaction of superoxide with anion of NTO is shown in Fig. 1. Nucleophilic addition to the carbon atoms of NTOa is unlikely to occur since the activation energy for this process is prohibitively high at room temperature (35-45 kcal/mol). A one-electron reduction of NTOa by superoxide is endergonic ($\Delta G_r = 3.05$ kcal/mol) and requires an activation energy of 7.68 kcal/mol. Proton transfer from superoxide to NTOa gives an adduct that lies 13.38 kcal/mol above

the reactants. Reactivity of NTOa is lower than reactivity of NTO in reaction with superoxide due to requirement of an additional activation energy to overcome the Coulomb repulsion between the two anionic species.

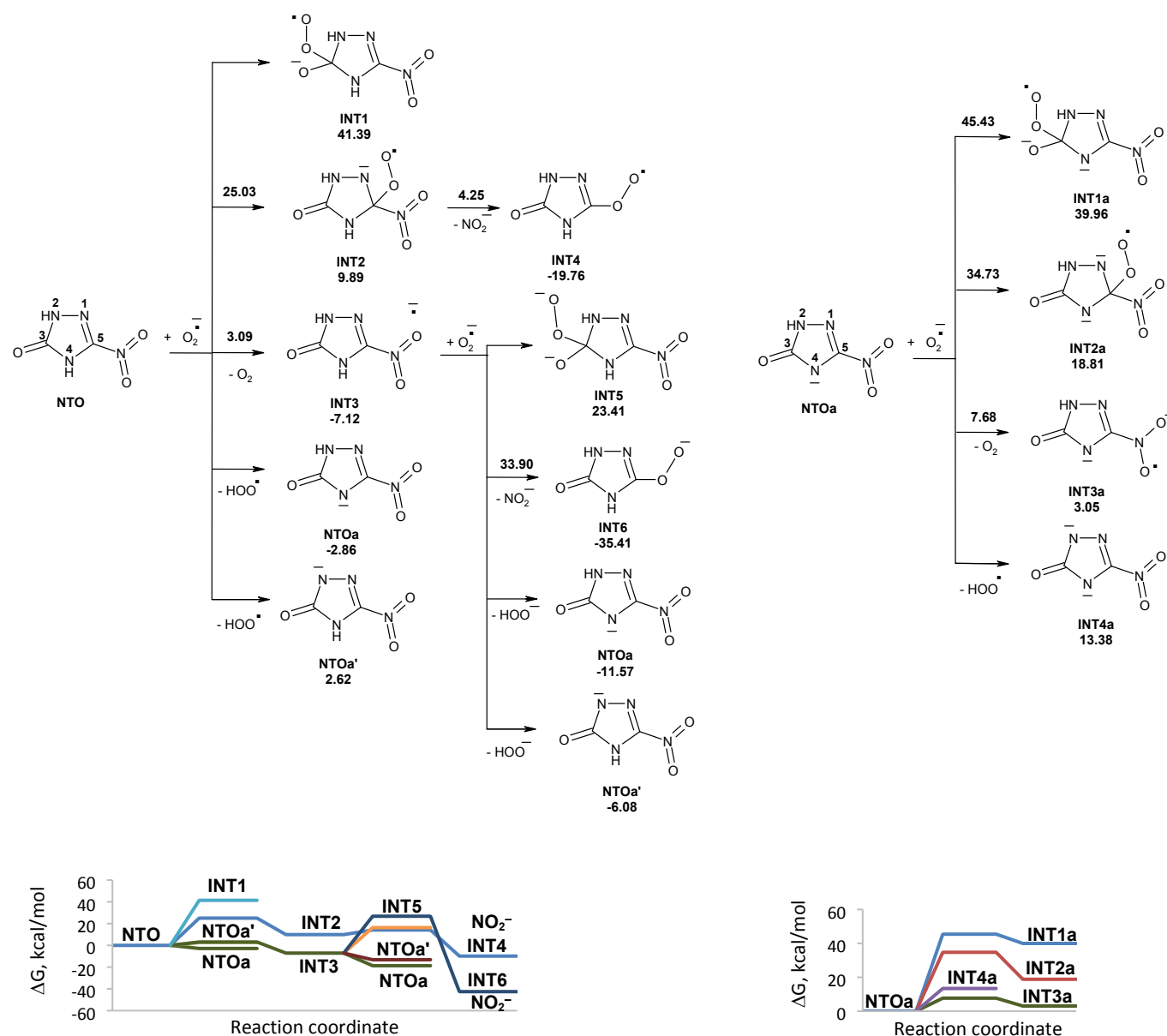


Fig. 1 PCM(Pauling)/M06-2X/6-311++G(d,p) modeled pathways for NTO and NTOa decomposition in water induced by superoxide along with the corresponding Gibbs free energy diagram. In the top figure, numbers along with each of the arrow indicate the corresponding reaction barrier height, while numbers below structures indicate the corresponding reaction Gibbs free energy in kcal/mol.

Reactivity of NTO in excited triplet state toward superoxide may differ from its reactivity in ground singlet state. An excitation of NTO in the environment that results in its singlet-triplet transformation may occur after absorption of sunlight. Modeled reactions of NTO* (in triplet state) with superoxide in water along with the corresponding Gibbs free energy diagram are shown in Fig. 2. Comparative analysis of energetic parameters for interaction of NTO and NTO* with superoxide showed that excitation significantly facilitates the studied processes (Figs. 1 and 2). The most favorable direction is barrierless attachment of superoxide to carbon atom C5 of NTO* that leads to INT2, which easily loses nitrite anion. Formed INT4 isomerizes into slightly more stable INT7. Cleavage of O-O bond in INT7 leads to cycle-opened intermediate INT9 via intermediate INT8. Hydroxyl radical, that was eliminated from INT7, may attack INT9. Hydrogen atom transfer from nitrogen atom of INT9 to hydroxyl radical has lower energy barrier than the addition of OH^\bullet to carbon atom of double bond $\text{C}=\text{O}$. Removal of hydrogen atom from INT9 is accompanied by cleavage of C-N bond and release of nitrogen gas and formation of INT11. Transformations of INT11 into intermediates INT14 and INT15 have similar energy barriers. An addition of molecule of water to INT11 leading to INT14 is more favorable due to the reaction is exergonic, while rupture of C-N bond in INT11 with elimination of carbon (II) oxide is endergonic. A transfer of hydrogen

atom from INT14 to superoxide occurs without activation energy and is accompanied by rupture of C-N bond with release of carbon (IV) oxide and isocyanic acid (INT16). Hydrolysis of isocyanic acid leads to intermediate INT17, which decomposes into ammonia and carbon (IV) oxide. Modeled pathways and Gibbs free energy calculations allow to suggest that degradation of NTO* in triplet state induced by superoxide in aqueous solution may lead to its mineralization with formation of nitrite anion, ammonia, nitrogen gas, and carbon (IV) oxide (Fig. 2).

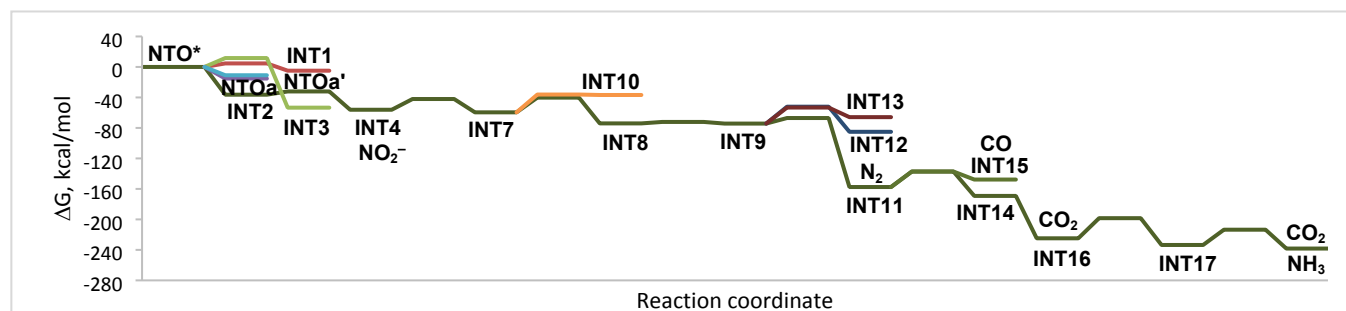
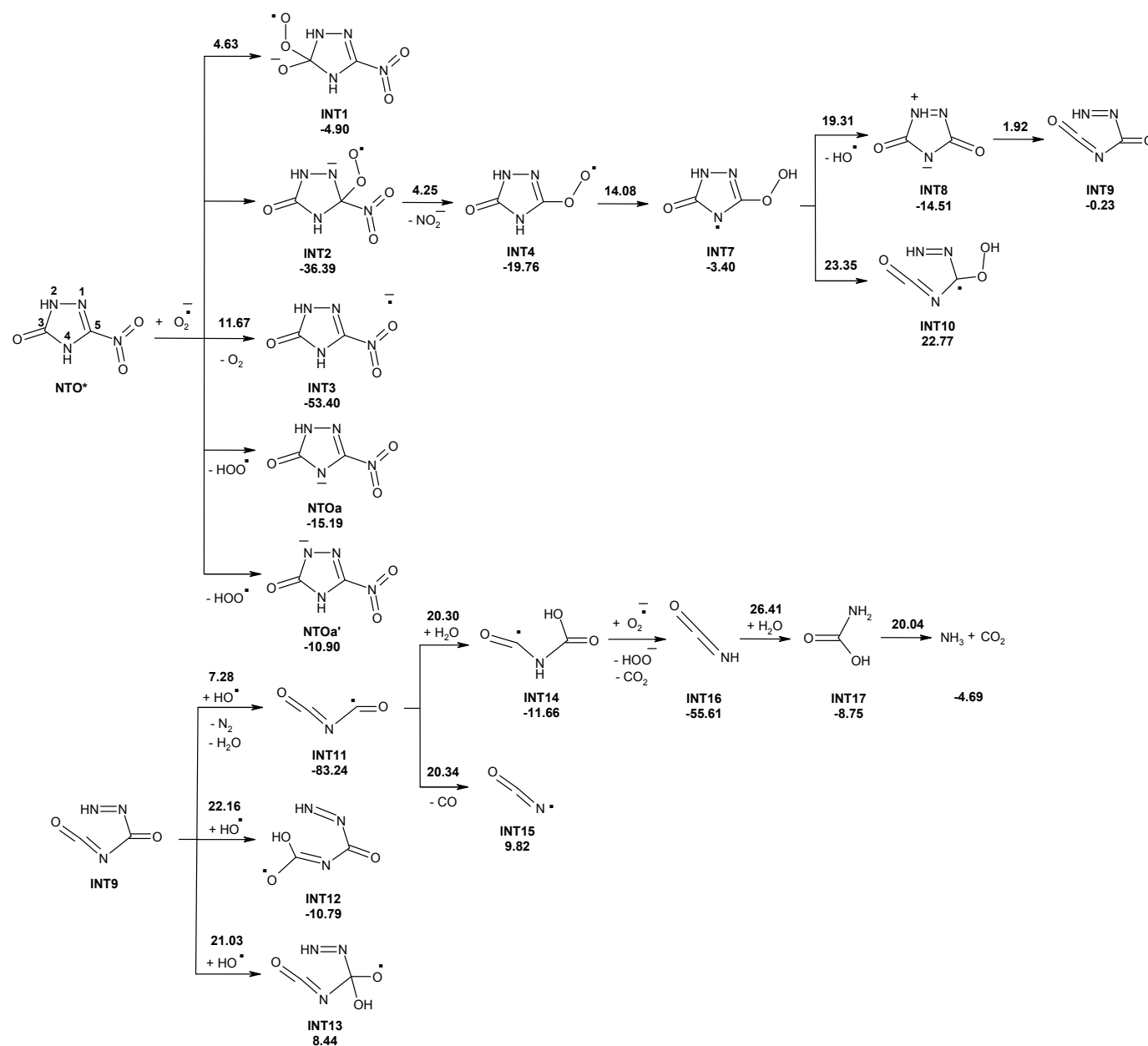


Fig. 2 PCM(Pauling)/M06-2X/6-311++G(d,p) modeled pathways for NTO* (triplet state) decomposition in water induced by superoxide along with the corresponding Gibbs free energy diagram. In the top figure, numbers along with each of the arrow indicate the corresponding reaction barrier height, while numbers below structures indicate the corresponding reaction Gibbs free energy in kcal/mol.

Reactions of NTOa* (in triplet state) with superoxide in water were also modeled (Fig. 3). Reactivity of NTOa in excited triplet state toward superoxide increases significantly as compared to one in ground singlet state (Figs. 1 and 3). The fastest processes are an electron transfer from superoxide to NTOa* and a proton transfer from NTOa* to superoxide. These processes lead to intermediates INT3a and INT4a, respectively. An attachment of superoxide to INT3a and INT4a is hard to occur due to high energy barriers of 33-45 kcal/mol. Instead, these intermediates may be easily transformed into NTOa (in singlet state) by electron and proton transfer, respectively. Thus, superoxide is unlikely to contribute to the degradation of NTOa (Figs. 1 and 3).

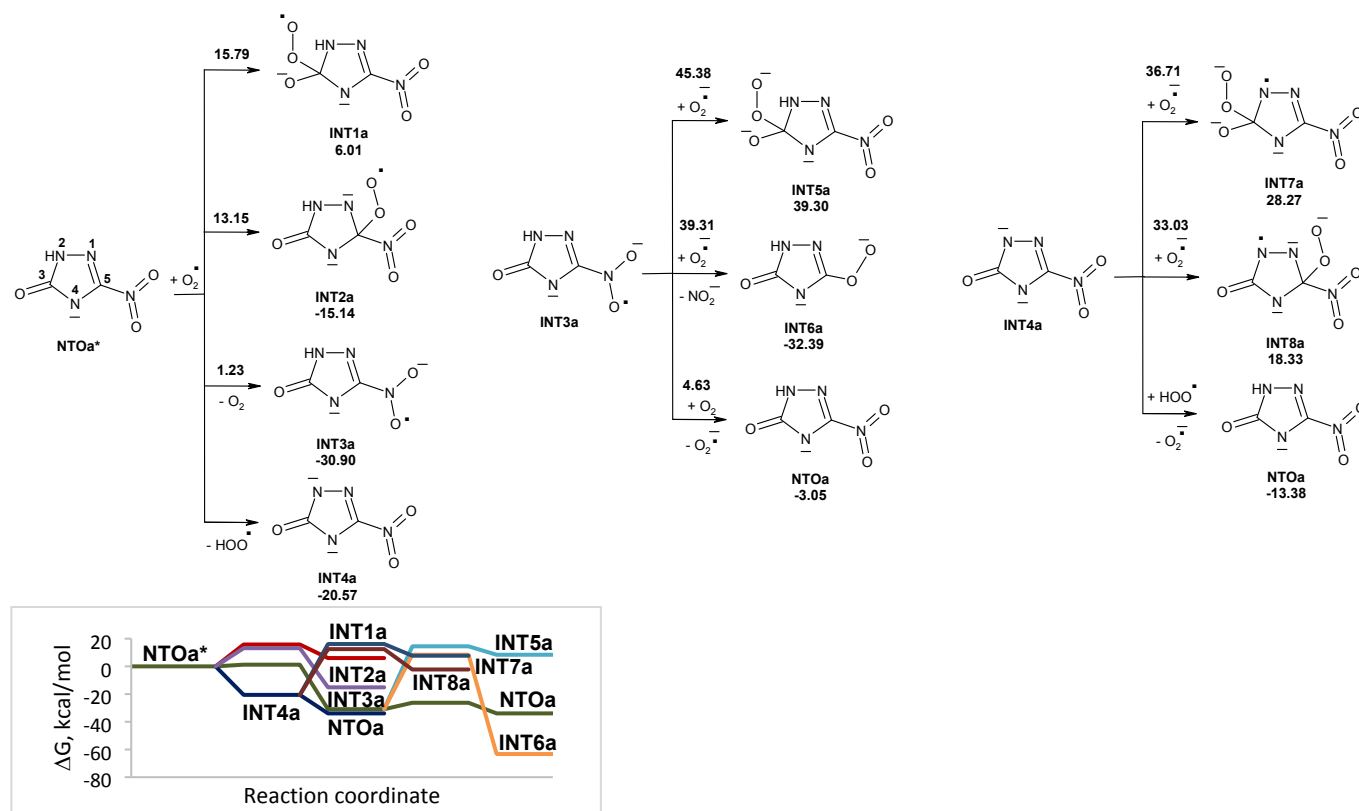


Fig. 3 PCM(Pauling)/M06-2X/6-311++G(d,p) modeled pathways for NTOa* (triplet state) decomposition in water induced by superoxide along with the corresponding Gibbs free energy diagram. In the top figure, numbers along with each of the arrow indicate the corresponding reaction barrier height, while numbers below structures indicate the corresponding reaction Gibbs free energy in kcal/mol.

Hydroperoxyl radical induced degradation of NTO and NTOa

Modeled pathways for NTO decomposition in water induced by hydroperoxyl radical along with the corresponding Gibbs free energy diagrams are shown in Fig. 4. Structures of the corresponding transition states are placed in Fig. S2 (ESI). The hydrogen atom transfer from NTO to HO₂[•], the hydroperoxyl radical attachment to carbon atoms of NTO, the one-electron reduction of NTO by HO₂[•] are endergonic processes. The addition of HO₂[•] to carbon atom C5 was found to be the most energy favorable pathway for the initial attack of HO₂[•] onto NTO with activation energy of 23.21 kcal/mol. The formed adduct INT2 undergoes fast transformation into INT4 by C-N bond rupture and release of nitrite radical. Interaction of nitrite radical with HO₂[•] results in formation of nitrous acid and oxygen gas. The reaction is exergonic and has activation energy of 17.91 kcal/mol. Elimination of a water molecule from INT4 leads to zwitterionic intermediate INT5 that undergoes nearly barrierless C-N bond rupture leading to cycle-opened intermediate INT6. Proton transfer between nitrogen atoms leads to decomposition of INT6 into isocyanic acid (INT10), carbon (II) oxide and nitrogen gas. The reaction is highly exothermic, however, activation barrier for the transfer is high to be realized at ambient temperature. An addition of water molecule to double bond C=O of INT6 may result in formation of intermediates INT7 and INT8. Hydrolytic rupture of C-N bond may lead to INT9 and N₂H₂. Transformation of INT6 into INT7 is the most kinetically favorable pathway with the lowest activation energy of 24.34 kcal/mol.

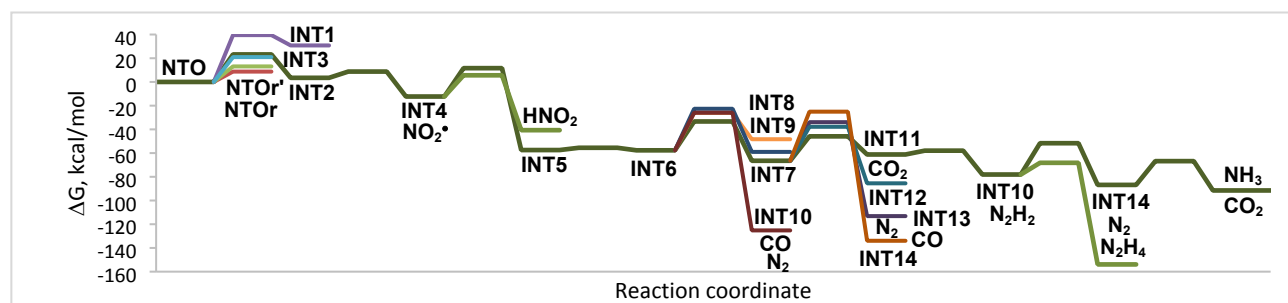
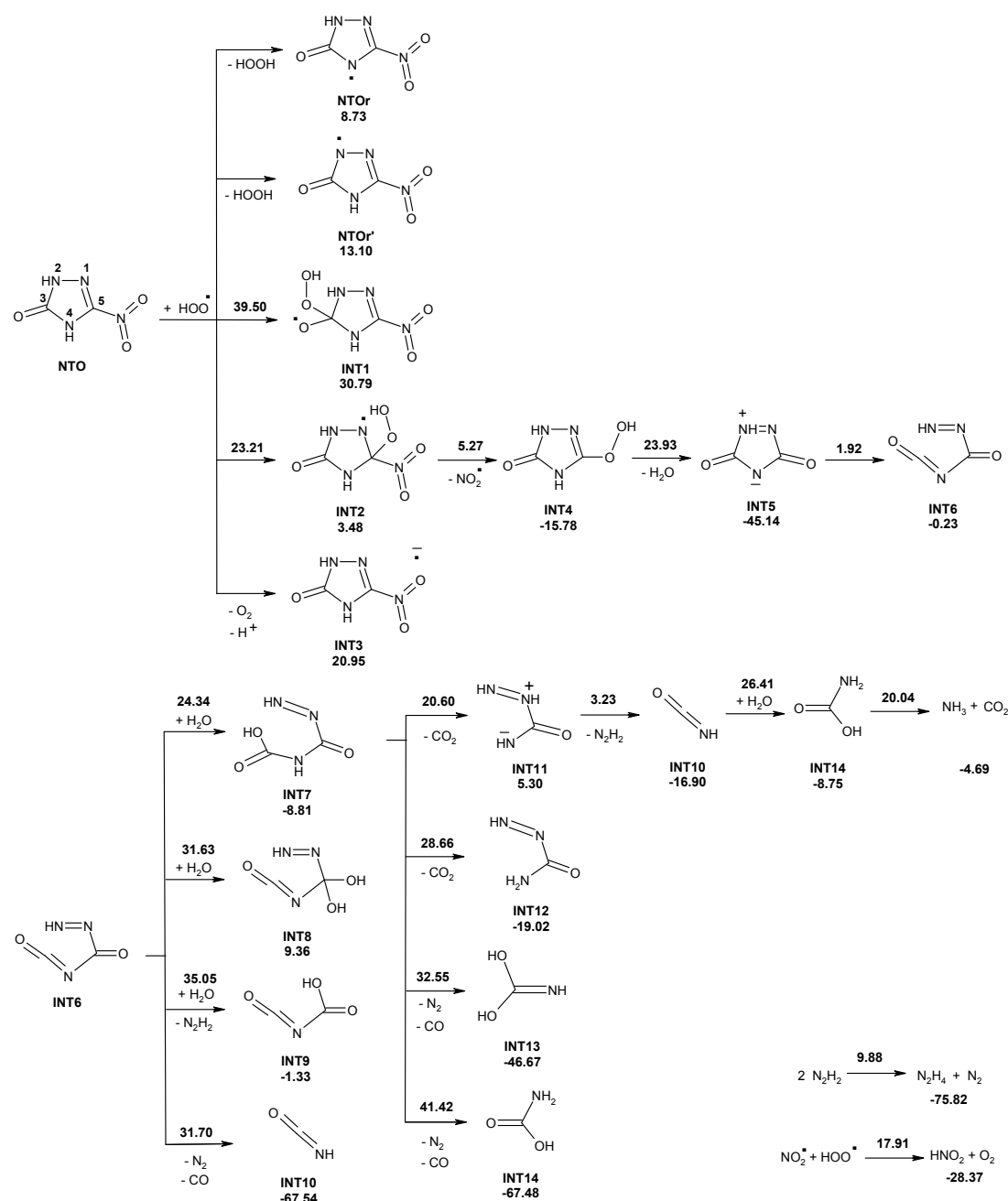


Fig. 4 PCM(Pauling)/M06-2X/6-311++G(d,p) modeled pathways for NTO decomposition in water induced by hydroperoxyl radical along with the corresponding Gibbs free energy diagram. In the top figure, numbers along with each of the arrow indicate the corresponding reaction barrier height, while numbers below structures indicate the corresponding reaction Gibbs free energy in kcal/mol.

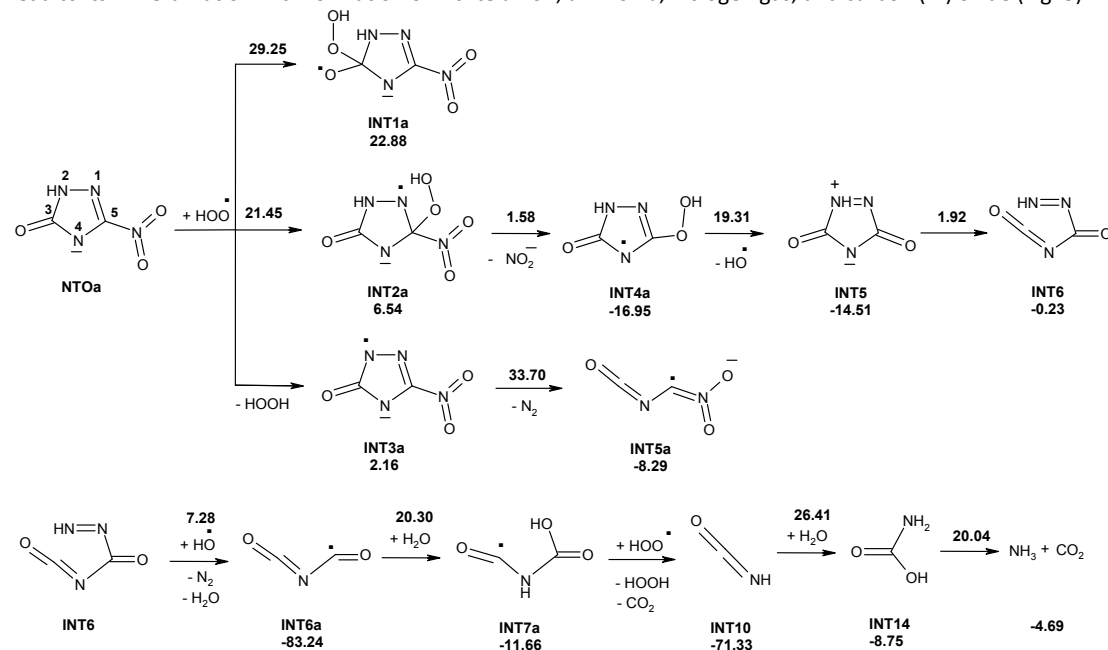
There are several pathways for unimolecular decomposition of INT7. Proton transfer from oxygen atom to nitrogen atom results in formation of INT11 and INT12 and elimination of carbon (IV) oxide. A proton transfer from nitrogen to oxygen atom leads to rupture of two C-N bonds and formation of INT13, nitrogen gas, and carbon (II) oxide. A proton transfer between two nitrogen atoms yields INT14, nitrogen gas, and carbon (II) oxide. Decomposition of INT7 into INT11 and CO₂ has the lowest activation barrier (20.60 kcal/mol) among the studied pathways. Despite the reaction is endergonic the intermediate INT11 undergoes nearly barrierless C-N bond rupture, which leads to the release of isocyanic acid (INT10) and N₂H₂. Hydrolysis of isocyanic acid proceeds via two steps and results in formation of ammonia and carbon (IV) oxide. Disproportionation reaction of N₂H₂ leads to hydrazine (N₂H₄) and nitrogen gas.

Modeled pathways and Gibbs free energy calculations allow to suggest that decomposition of NTO induced by hydroperoxyl radical in aqueous solution may lead to its mineralization (Fig. 4). Predicted products are nitrous acid, ammonia, nitrogen gas, hydrazine and carbon (IV) oxide. There are a few steps with activation energy more than 20 kcal/mol along the most energy favorable reaction channel. We suggest that use of additional water molecules for calculation may stabilize transition states and reduce activation energy. The slowest step in NTO decomposition is a hydrolysis of isocyanic acid with activation barrier of more than 26 kcal/mol. In the recent work we showed that acidic catalysis may considerable decrease the activation energy for the hydrolysis of isocyanic acid to 9.51 kcal/mol.¹⁰

An attachment of hydroperoxyl radical appears to be more energy favorable than an attachment of superoxide to carbon atom C5 of NTO (Figs. 1,4). Relatively higher rate of hydroperoxyl radical trapping as compared to that of superoxide was earlier demonstrated for nitrone 5,5-dimethyl-1-pyrroline *N*-oxide by comparative analysis of Gibbs free activation energy of O₂^{•−} or HO₂[•] addition to C=N double bond of the nitrone in aqueous system.¹⁹

Modeled pathways for decomposition of anion of NTO in water induced by hydroperoxyl radical along with the corresponding Gibbs free energy diagrams are shown in Fig. 5. Reaction of hydroperoxyl radical with NTOa starts from an addition of HO₂[•] to carbon atom C5 of C5=N1 double bond, that was found to be more energy favorable pathway than the initial attack of HO₂[•] onto C3 atom of NTOa. Formed INT2a is less stable than reactants, however the intermediate fast transforms into more stable INT4a by release of nitrite anion. The activation energy for the interaction of hydroperoxyl radical with NTOa is lower than for the reaction of HO₂[•] with NTO that suggests higher reactivity of deprotonated anionic form of NTO toward a hydroperoxyl radical. That is confirmed by smaller value of energy gap between the frontier molecular orbitals of NTOa and HO₂[•] (7.92 eV), than between ones of NTO and HO₂[•] (8.65 eV). An alternative reaction pathway of initial transformation of NTO anion involving a hydrogen atom transfer from NTOa to HO₂[•] is slightly endergonic and further decomposition of INT3a requires high activation energy that suggests this direction of NTOa transformation is hard to occur.

Cleavage of O-O bond in INT4a leads to intermediate INT5 and hydroxyl radical. The cycle opening in INT5 leads to intermediate INT6, which may be attacked by hydroxyl radical. A transfer of hydrogen atom from nitrogen atom of INT6 to hydroxyl radical is accompanied by cleavage of C-N bond and release of nitrogen gas and formation of INT6a. An addition of molecule of water to INT6a results in formation of INT7a. Hydroperoxyl radical captures hydrogen atom from INT7a without activation barrier that leads to rupture of C-N bond with release of carbon (IV) oxide and isocyanic acid (INT10). Two-step hydrolysis of isocyanic acid yields ammonia and carbon (IV) oxide. Modeled pathways and Gibbs free energy calculations allow to suggest that degradation of anion of NTO induced by hydroperoxyl radical in aqueous solution may lead to its mineralization with formation of nitrite anion, ammonia, nitrogen gas, and carbon (IV) oxide (Fig. 5).



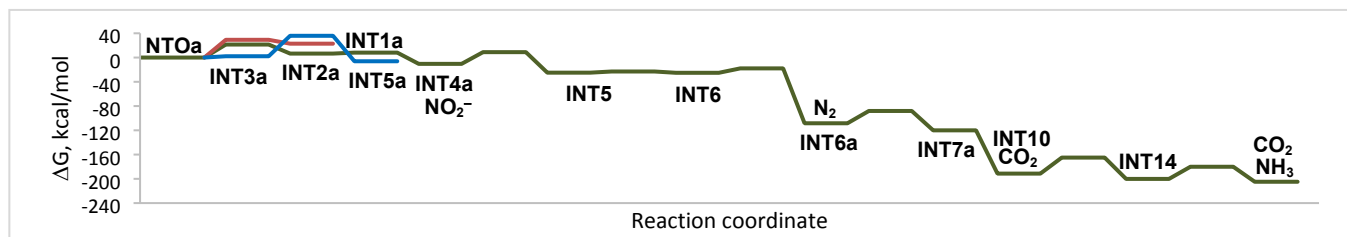
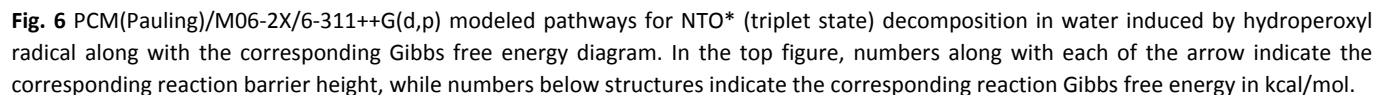


Fig. 5 PCM(Pauling)/M06-2X/6-311++G(d,p) modeled pathways for NTOa decomposition in water induced by hydroperoxyl radical along with the corresponding Gibbs free energy diagram. In the top figure, numbers along with each of the arrow indicate the corresponding reaction barrier height, while numbers below structures indicate the corresponding reaction Gibbs free energy in kcal/mol.

Modeled pathways for degradation of NTO* and NTOa* in triplet state induced by hydroperoxyl radical are shown in Figs. 6 and 7, respectively. Excitation of NTO and NTOa makes the addition of hydroperoxyl radical hard to occur due to high activation energy. Barrierless capture of hydrogen atom from NTO* by HO₂* leads to more stable intermediates NTO[•] and NTO[•] than an electron transfer from hydroperoxyl radical to NTO*, leading to INT3 (Fig.6). Radical intermediate NTO[•] is more stable than NTO[•] and may undergo an attachment of molecule of water with formation of INT18. An addition of hydroperoxyl radical to NTO[•] requires higher activation energy than an addition of water molecule. An attack of water molecule onto carbon atom C5 is more favorable than the one onto atom C3. Intermediate INT18 easily loses nitrite radical, which may transform into nitrous acid by fast capturing hydrogen from INT21. Decomposition of INT22 into isocyanic acid (INT10) and INT28 as well as an addition of hydroperoxyl radical to INT22 will not occur due to high activation energy and endergonicity. A hydrogen transfer from INT22 to hydroperoxyl radical is a barrierless process leading to INT5, which undergoes rapid opening of five-membered cycle. An addition of molecules of water to INT6 results in sequential release of carbon (IV) oxide, diimide and ammonia. Diimide can go through a disproportionation reaction to form nitrogen gas and hydrazine (Fig.4).

Comparative analysis of NTO degradation in water induced by hydroperoxyl radical for singlet and triplet states of NTO showed that in both cases NTO undergoes complete mineralization into nitrous acid, nitrogen gas, ammonia and carbon (IV) oxide (Figs. 4 and 6). An initial reaction of NTO with hydroperoxyl radical is an addition of HO₂* to carbon atom C5 of NTO. Excitation of NTO considerably increases the activation energy for the addition reaction, making a hydrogen transfer from NTO* to hydroperoxyl radical the most favorable initial reaction. Further transformations of INT1 (Fig.4) and NTO[•] (Fig.6) lead to INT5, and then the degradation proceeds by the same way for the both cases.



Excitation of NTOa also facilitates a hydrogen transfer from NTOa* to hydroperoxyl radical (Fig.7). However, formed INT3a may capture a hydrogen from hydrogen peroxide, that results in formation of NTOa in singlet state. Other possible decomposition pathway for INT3a, that is release of nitrogen gas and formation of INT5a (Fig.5), was ruled out due to high activation barriers. Thus, hydroperoxyl radical can contribute in degradation of NTOa in its singlet state (Fig.5).

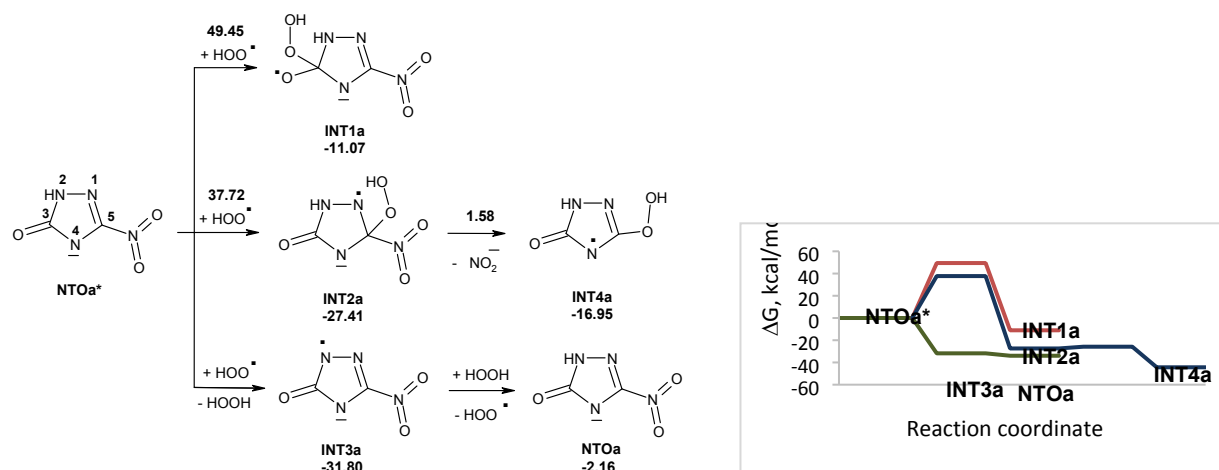


Fig. 7 PCM(Pauling)/M06-2X/6-311++G(d,p) modeled pathways for NTOa* (triplet state) decomposition in water induced by hydroperoxyl radical along with the corresponding Gibbs free energy diagram. In the top figure, numbers along with each of the arrow indicate the corresponding reaction barrier height, while numbers below structures indicate the corresponding reaction Gibbs free energy in kcal/mol.

The current study established that superoxide and hydroperoxyl radical may take an active part in the process of NTO degradation. Superoxide mainly participates in deprotonation of NTO in singlet state. Excitation of NTO facilitates its degradation induced by superoxide, that may result in complete mineralization of NTO. The degradation pathway consists of an addition of superoxide to carbon atom of NTO, release of nitrite anion, cleavage of five-membered cycle, elimination of nitrogen gas, hydrolysis leading to formation of carbon (IV) oxide and ammonia. Hydroperoxyl radical appears to be more reactive than superoxide in reaction with NTO (in singlet state) on the basis of the calculated Gibbs free activation energies. Decomposition of NTO induced by hydroperoxyl radical in water is a multistep process, which leads to mineralization of the studied nitrocompound. The initial nucleophilic addition of HO_2^\bullet to NTO occurs at the carbon atom of double bond $\text{C}=\text{N}$. Then sequential transformations occur involving release of nitrite radical, cycle opening, water molecule addition, breaking of $\text{C}-\text{N}$ bonds. Predicted products are nitrous acid, ammonia, nitrogen gas, hydrazine, and carbon (IV) oxide. Degradation of NTO anion induced by hydroperoxyl radical resulted in formation of nitrite anion, nitrogen gas, carbon (IV) oxide, and ammonia. Excitation of NTO causes change of an initial step of reaction between NTO and hydroperoxyl radical toward formation of NTO radical. An addition of molecules of water to the NTO radical leads to release of nitrite radical, which then transforms into nitrous acid, diimide, which may form nitrogen gas and hydrazine, carbon (IV) oxide and ammonia. Formation of nitrous acid (nitrite anion), ammonia, and carbon (IV) oxide are experimentally observed during photolytic decomposition of NTO in aqueous solution.³⁻⁸

Conclusions

Superoxide and hydroperoxyl radical are important reactive oxygen species produced in the aquatic environment under sunlight irradiation. They may cause decomposition of organic pollutants. The ability of superoxide and hydroperoxyl radical to take part in degradation of NTO was studied at the PCM/M06-2X/6-311++G(d,p) theory level. Our results revealed that superoxide fast deprotonates NTO, while hydroperoxyl radical may cause mineralization of NTO. Degradation of NTO induced by hydroperoxyl radical proceeds through several steps, starting from hydroperoxyl attachment to carbon atom of $\text{C}=\text{N}$ double bond of NTO. Sequential cleavage of $\text{C}-\text{N}$ bonds and addition of water molecules leads to such products of NTO degradation as nitrous acid, ammonia, nitrogen gas, hydrazine, and carbon (IV) oxide. Anionic form of NTO is more reactive toward interaction with hydroperoxyl radical as compared with its neutral form. An absorption of UV-irradiation under environmentally relevant conditions causes singlet-triplet transformation of NTO, that significantly affects its reactivity. In the reaction of triplet NTO with superoxide, the corresponding activation barriers are lowered, that allows to start a sequence of processes to achieve complete mineralization of NTO. Based on the energetics of the studied reaction pathways we suggest that indirect photolysis induced by hydroperoxyl radical and superoxide may contribute to NTO degradation in environment.

Author Contributions

All authors have read and agreed to the published version of the manuscript.

Conflicts of interest

There are no conflicts to declare.

Acknowledgements

We thank ARO for financial support (grant number is W911NF-20-1-0116). The computation time was provided by the Mississippi Center for Supercomputer Research. The use of trade, product, or firm names in this report is for descriptive purposes only and does not imply endorsement by the U.S. Government. The findings of this report are not to be construed as an official Department of the Army position unless so designated by other authorized documents.

Notes and references

- 1 R. J. Spear, C. N. Louey and M. G. Wolfson, *A preliminary assessment of 3-nitro-1,2,4-triazol-5-one (NTO) as an insensitive high explosive*, DSTO Materials Research Laboratory, Maribyrnong, Australia, 1989.
- 2 S. Taylor, E. Park, K. Bullion and K. Dontsova, *Chemosphere* 2015, **119**, 342–348.
- 3 K. Dontsova, S. Taylor, R. Pesce-Rodriguez, M. Brusseau, J. Arthur, N. Mark, M. Walsh, J. Lever and J. Simunek, *Dissolution of NTO, DNAN, and insensitive munitions formulations and their fates in soils, ERDC/CRREL TR-14-23*, Hanover, NH, 2014.
- 4 A. Halasz, J. Hawari and N. N. Perreault, *Environ. Sci. Technol.*, 2018, **52**, 589–596.
- 5 J. B. Becher, S. A. Beal, S. Taylor, K. Dontsova and D. E. Wilcox, *Chemosphere*, 2019, **228**, 418–426.
- 6 L. C. Moores, S. J. Jones, G. W. George, D. L. Henderson, T. C. Schutt, *J. Photochem. Photobiol. A: Chem.*, 2020, **386**, 112094.
- 7 L. C. Moores, A. J. Kennedy, L. May, S. M. Jordan, A. J. Bednar, S. J. Jones, D. L. Henderson, L. Gurtowski and K. A. Gust, *Chemosphere*, 2020, **240**, 124958.
- 8 H. W. Schroer, E. Londono, X. Li, H. J. Lehmler, W. Arnold, C. L. Just, *ACS ES T Water*, 2023, **3**(3), 783–792.
- 9 L. K. Sviatenko, L. Gorb and J. Leszczynski, *Struct. Chem.*, 2023, **34**, 23–31.
- 10 L. K. Sviatenko, L. Gorb and J. Leszczynski, *Phys. Chem. A*, 2023, **127**(12), 2688–2696.
- 11 R. M. Baxter and J. H. Carey, *Nature*, 1983, **306**, 575–576.
- 12 B. H. J. Bielski, D. E. Cabelli, R. L. Arudi and A. B. Ross, *J. Phys. Chem. Ref. Data.*, 1985, **14**, 1041–1100.
- 13 D. S. Dimic, D. A. Milenkovic, E. H. Avdovic, D. J. Nakarada, J. M. Dimitric Markovic and Z. S. Markovic, *Chem. Eng. J.*, 2021, **424**, 130331.
- 14 W. H. Koppenol and J. Butler, *Adv. Free Radic. Biol. Med.*, 1985, **1**(1), 91–131.
- 15 D. Behar, G. Czapski, J. Rabani, L. M. Dorfman and H. A. Schwarz, *J. Phys. Chem.*, 1970, **74**(17), 3209–3213.
- 16 V. S. Bryantsev, V. Giordani, W. Walker, M. Blanco, S. Zecevic, K. Sasaki, J. Uddin, D. Addison and G. V. Chase, *J. Phys. Chem. A*, 2011, **115**(44), 12399–12409.
- 17 D. T. Usmanov, S. Ninomiya, K. Hiraoka and S. Yamabe, *Int. J. Mass Spectrom.*, 2020, **450**, 116308.
- 18 Z. Dhaouadi, M. Nsangou, N. Garrab, E. H. Anouar, K. Marakchi and S. Lahmar, *J. Mol. Struct.: THEOCHEM*, 2009, **904**(1–3), 35–42.
- 19 F. A. Villamena, J. K. Merle, C. M. Hadad and J. L. Zweier, *J. Phys. Chem. A*, 2005, **109**(27), 6083–6088.
- 20 L. K. Sviatenko, L. Gorb, D. Leszczynska, S. I. Okovytyy, M. K. Shukla and J. Leszczynski, *J. Phys. Chem. A*, 2019, **123**, 7597–7608.
- 21 M. J. Frisch, G. W. Trucks, H. B. Schlegel, G. E. Scuseria, M. A. Robb, J. R. Cheeseman, G. Scalmani, V. Barone, B. Mennucci, G. A. Petersson, et al. Gaussian 09, Revision A.01.; Gaussian, Inc.: Wallingford CT, 2009.
- 22 Y. Zhao and D. G. Truhlar, *Theor. Chem. Account*, 2008, **120**, 215–241.
- 23 Y. Zhao and D. G. Truhlar, *J. Chem. Phys.*, 2006, **125**, 194101–194118.
- 24 S. F. Sousa, P. A. Fernandes and M. J. Ramos, *J. Phys. Chem. A*, 2007, **111**, 10439–10452.
- 25 W. J. Hehre, L. Radom, P. R. Schleyer and J. A. Pople, *Ab Initio Molecular Orbital Theory*, Wiley, New York, USA, 1986.
- 26 M. Cossi, V. Barone, R. Cammi and J. Tomasi, *Chem. Phys. Lett.*, 1996, **255**, 327–335.
- 27 R. A. Marcus, *Rev. Mod. Phys.*, 1993, **65**, 599–610.
- 28 L. K. Sviatenko, L. Gorb, D. Leszczynska, S. I. Okovytyy, M. K. Shukla and J. Leszczynski, *Struct. Chem.*, 2021, **32**, 521–527.